Running Title: Systemic induction of photosynthesis

Corresponding author:
Yanhong Zhou
Department of Horticulture, Zijingang Campus, Zhejiang University, 866 Yuhangtang Road, Hangzhou 310058, China.

Telephone: 0086-571-88982276
Fax: 0086-571-88982276
E-mail address:yanhongzhou@zju.edu.cn

Research area: Signaling and Response

Title: Systemic induction of photosynthesis via illumination of the shoot apex is mediated sequentially by phytochrome B, auxin and hydrogen peroxide in tomato

Authors: Zhixin Guo[1], Huizi Li[1], Xun Xiang[1], Golam Jalal Ahammed[1], Mengmeng Wang[3], Eugen Onac[3], Jie Zhou[1], Xiaojian Xia[1], Kai Shi[1], Jingquan Yu[1,2], Christine H. Foyer[4], and Yanhong Zhou[1,2,*]

[1]*Department of Horticulture, Zijingang Campus, Zhejiang University, 866 Yuhangtang Road, Hangzhou, 310058, P.R. China*

[2]*Zhejiang Provincial Key Laboratory of Horticultural Plant Integrative Biology, 866 Yuhangtang Road, Hangzhou, 310058, P.R. China*

[3]*Philips Research Europe, High Tech Campus 34, 5656 AE Eindhoven, Netherlands*

[4]*Centre for Plant Sciences, Faculty of Biology, University of Leeds, Leeds, LS2 9JT, UK*

One sentence summary:

Red light perceived in the shoot apex by phyB alters IAA and H_2O_2 signaling in a systemic manner, leading to accelerated photosynthetic induction in systemic leaves, by increasing cyclic electron flow-dependent ATP production

Footnotes:

List of author contributions

Y.Z. and J.Y. designed the research; Z.G., H.L., and X.X. performed the research; all authors analyzed the data; G.A., M.W., E.O., J.Z., X.X., and K.S. discussed the data; Y.Z., J.Y. and C. H. F wrote the article with contributions from the other authors.

[1]**Funding information:** This work was supported by the National Natural Science Foundation of China (grant nos. 31372109, 31430076), the Special Fund for Agro-scientific Research in the Public Interest (201203004), the Fundamental Research Funds for the Central Universities (2016XZZX001-07), the National High Technology R & D Program of China (2013AA102406), and the Fok Ying-Tong Education Foundation (132024).

*Corresponding author; email yanhongzhou@zju.edu.cn

ACKNOWLEDGMENTS

We are grateful to the Tomato Genetics Resource Center at the California University for tomato phytochrome mutants. We thank Dr. Ivanchenko of Oregon State University for providing *dgt* seeds. Thanks to Xiaodan Wu (Analysis Center of Agrobiology and Environmental Sciences, Institute of Agrobiology and Environmental Sciences, Zhejiang University) for assistance with phytohormones analysis.

ABSTRACT

Systemic signaling of upper leaves promotes the induction of photosynthesis in lower leaves allowing more efficient use of light flecks. However, the nature of the systemic signals has remained elusive. Here we show that pre-illumination of the shoot apex alone can accelerate photosynthetic induction in distal leaves and that this process is light-quality dependent, where red light promotes and far red light delays photosynthetic induction. Grafting the wild type (WT) rootstock with a *phyB* mutant scion compromised light-induced photosynthetic induction, as well as auxin biosynthesis in the shoot apex, auxin signaling and *RESPIRATORY BURST OXIDASE HOMOLOG 1* (*RBOH1*)-dependent H_2O_2 production in the systemic leaves. Light-induced systemic H_2O_2 production in the leaves of the rootstock was also absent in plants grafted with an auxin resistant *dgt* mutant scion. Cyclic electron flow around photosystem I and associated ATP production were increased in the systemic leaves by exposure of the apex to red light. This enhancement was compromised in the systemic leaves of the WT rootstock with *phyB* and *dgt* mutant scions and also in *RBOH1*-RNAi leaves with the WT as scion. Silencing of *ORR*, which encodes NAD(P)H dehydrogenase, compromised the systemic induction of photosynthesis. Taken together, these results demonstrate that exposure to red light triggers phyB-mediated auxin synthesis in the apex leading to H_2O_2 generation in systemic leaves. Enhanced H_2O_2 levels in turn activate cyclic electron flow and ATP production, leading to a faster induction of photosynthetic CO_2 assimilation in the systemic leaves allowing plants better adaptation to the changing light environment.

Keywords: auxin, cyclic electron flow, H_2O_2, photosynthesis, phytochrome B, RBOH1, systemic signaling

INTRODUCTION

As a consequence of their sessile lifestyle, plants have evolved a high capacity for regulation of physiology, growth and development that facilitates survival in a constantly changing environment. Environmental stimuli perceived within each organ not only influence morphogenetic and physiological changes within that organ but also generate systemic effects in other organs that are remote from the site of signal perception. This crucial phenomenon is called systemic signaling or systemic regulation. Systemic signaling prepares other tissues of a plant for future challenges that may initially only be sensed by a few local tissues or cells. Several types of systemic responses are known. These include systemic acquired resistance (SAR) that is typically activated by pathogens such as viruses, bacteria and fungi (Fu and Dong, 2013), induced systemic resistance (ISR) that is triggered by beneficial soil microorganisms or others (Pieterse and Dicke, 2007), and systemic acquired acclimation (SAA) that is initiated by abiotic stresses such as high light, ultraviolet radiation, heat, cold and salinity (Mittler and Blumwald, 2015).

The light utilization efficiency of photosynthesis is important for the survival of understory plants and plants growing in canopies. In particular, the efficient use of the energy contained in light (sun) flecks is important because light flecks contribute up to 60–80% of photosynthetically active radiation (PAR) received by understory plants (Pearcy and Seemann, 1990; Leakey et al., 2003; 2005). Earlier studies have shown the existence of systemic regulation of stomatal development and of photosynthesis in developing leaves in response to environmental signals perceived by mature leaves such as changing irradiance and atmospheric CO_2 conditions (Lake et al., 2002; Coupe et al., 2006; Araya et al., 2008). Phytochome(phy)B is important in the transmission of the systemic signals that modulate stomatal development in young leaves of Arabidopsis (Casson et al., 2014). In tomato, there are two forms of phyB, phyB1 and phyB2, that work together to mediate red light-induced responses, such as hypocotyl elongation and greening in seedlings (Hauser et al. 1995; Weller et al. 2000).

Photosynthesis is completely switched off in the dark, specifically to prevent futile cycling of metabolites through the reductive and oxidative pentose phosphate pathways. Hence, leaves need time to reactivate the enzymes of carbon assimilation

after a period of darkness. The time taken to reach maximum net rates of photosynthesis upon illumination is called photosynthetic induction (Walker, 1973). Systemic signaling has also been observed for the regulation of photosynthesis in relation to leaf ontology in understory plants (Montgomery and Givnish, 2008). The uppermost leaves, which are generally the first to receive sunlight, display faster photosynthetic induction times than understory leaves (Bai et al., 2008). Photosynthetic induction in understory leaves is enhanced by pre-illumination of upper leaves but not by lower leaves suggesting a directional signal transfer (Hou et al., 2015). While this process allows plants to use the light energy in sun flecks more efficiently, the nature of the systemic signals and their transmission pathways remain largely unresolved. Although, systemic signalling between different leaf ranks has been suggested to occur through the xylem (Thorpe et al., 2007), and also via electrical signals (Zimmermann et al., 2009), it is likely that systemic signals also pass through the phloem (Turgeon and Wolf, 2009; Hou et al., 2015). In addition, the phytohormone auxin is produced in the shoot apex and redistributed throughout the shoot by rapid non-polar phloem transport (Ljung et al., 2001). Changes in the light environment can dramatically alter auxin homeostasis, which is regulated in a light quality- and photoreceptor-dependent manner (Halliday et al., 2009).

The photosynthetic electron transport chain exhibits enormous flexibility in the relative rates of NADPH and ATP production, in order to accommodate the varying requirements of metabolism (Foyer et al., 2012). Non-cyclic, pseudocyclic and cyclic electron flow (CEF) pathways operate in the photosynthetic electron transport chain to drive the proton gradient across the thylakoid membrane (Allen, 2003). Photosynthetic induction is not only associated with the activation of the light- and thiol-dependent activation of carbon assimilation enzymes but also dependent on a high rate of CEF to drive ATP synthesis (Foyer and Harbinson, 1992). Considerable over-reduction of the electron transport acceptors occurs during the photosynthetic induction period and this continues until carbon assimilation can be activated. CEF around photosystem I (PSI), an essential component of photosynthesis, drives the proton gradient in a situation when NADP reduction has reached highest capacity and this essential electron acceptor is no longer available (Yamori et al., 2015; 2016). CEF is particularly sensitive to the reduction-oxidation (redox) status of the chloroplast, which is in turn responsive to cellular redox homeostasis. Oxidants, such as hydrogen peroxide, which are produced by pseudocyclic electron flow in the chloroplasts, play

a crucial role in the activation of CEF through modulation of the activity of the NADPH-plastoquinone reductase complex (Strand et al., 2015). Hormone-mediated generation of hydrogen peroxide can also stimulate CO_2 assimilation (Jiang et al., 2012).

Auxins, such as indole-3-acetic acid (IAA) generate hydrogen peroxide (Ivanchenko et al., 2013; Peer et al., 2013) and can regulate CO_2 assimilation (Bidwell and Turner, 1966; Hayat et al., 2009; Peng et al., 2013). We therefore used tomato plants to test the hypothesis that the systemic signaling that regulates photosynthetic induction in understory leaves arises from light-induced changes in auxin and H_2O_2 homeostasis involving modulation of CEF in systemic leaves. We present evidence showing that red light perceived in the shoot apex by a phyB–dependent pathway alters IAA signaling, in a systemic manner. IAA signals from the apex perceived in distal leaves, trigger systemic H_2O_2 production that accelerates photosynthetic induction by increasing CEF-dependent ATP production in the systemic leaves. These findings provide new insights into the elaborate plant regulatory network that allows light-adaptation in different organs.

RESULTS

Systemic Induction of Photosynthesis in the Distal Leaves of Tomato Plants is Dependent on Phytochrome B in the Shoot Apex

The following experiments were performed in order to examine the effects of light perceived by in the apex on the physiological functions of distal leaves. In particular, we focused on the induction of photosynthesis in distal leaves. Therefore, the shoot apex only was exposed to white light (WL) at an intensity of 300 μmol m^{-2} s^{-1} for 30 min whilst other leaves were left in the dark (Supplemental Fig. S1). The induction of photosynthesis was then measured in the 4th leaves on the stem below the apex upon exposure to high light (1500 μmol m^{-2} s^{-1} photosynthetic photon flux density, PPFD)for 30 min. A pre-illumination of either the uppermost fully expanded (1st to 3rd leaves) or the lower leaves (5-6th leaves) on the stem did not significantly change the time required to reach 50% (T50) and 90% (T90) of the maximal CO_2 assimilation rates in the 4th leaves (systemic leaf, SL) (Fig. 1B). In contrast, exposure of the apex to WL for 30 min resulted in a faster induction of CO_2 assimilation in the 4th leaves, compared to the dark controls. The T50 and T90 of the maximal CO_2 assimilation rates were decreased from 8.17 min to 4.30 min and from 19.7 min to 14.7 min,

respectively (Fig. 1, A and B). However, the increased induction of photosynthesis was only observed when the PPFD applied was higher than the light compensation point (ca. 50 μmol m^{-2} s^{-1}; Supplemental Fig. S2). These findings demonstrate that only the light perceived by the shoot apex was able to transmit systemic signal(s) to the systemic leaves in order to facilitate a more rapid induction of CO_2 assimilation.

To determine the nature of the signals that facilitate a more rapid induction of CO_2 assimilation in the systemic leaves, we applied red (R, 660 nm) and far-red (FR, 735 nm) light at an intensity of 300 μmol m^{-2} s^{-1} to the shoot apex for 30 min prior to the measurement of the induction of CO_2 assimilation in the distal (4^{th}) leaves (Supplemental Fig. S1). R light enhanced photosynthetic induction while FR light delayed the induction of CO_2 assimilation in the 4^{th} leaves (Fig. 1C). Interestingly, R light-induced photosynthesis was abolished when R light was supplemented with FR light at R/FR ratios of 1:1 or 1:2, but the stimulation of photosynthetic induction was still observed at R/FR of 2:1 (Fig. 1D). Moreover, reciprocal R /FR light exposures at 5 min-intervals for up to 6 cycles failed to enhance the rate of photosynthetic induction (Fig. 1E). We then grafted the young shoots of wild type (WT) tomatoes, tomato mutants deficient in phytochrome A *(phyA*), phytochrome B1 and B2 (*phyB1B2*) or cryptochrome 1 (*cry1*) with two developing leaves onto stems of WT plants with four leaves. This resulted in 4 grafting combinations: WT/WT, *phyA*/WT, *phyB1B2*/WT and *cry1*/WT, respectively. As had been observed in the WT plants, a pre-illumination with WL for 30 min resulted in a faster induction of CO_2 assimilation in the rootstock leaves (4^{th} leaf) of the WT/WT, *phyA*/WT and *cry1*/WT plants compared to dark controls (Fig. 1F; Supplemental Fig. S3 and 4). In contrast, the WL-dependent induction of CO_2 assimilation was compromised in *phyB1B2*/WT plants which showed little change in the T50 and T90 values compared to the leaves of the WT (Fig. 1F; Supplemental Fig. S4). However, chlorophyll content in the developing leaves of *phyB1B2* was not significantly different from those in WT plants (data not shown). This finding demonstrates that phyB signaling in the apex plays a critical role in the enhancement of photosynthetic induction in distal systemic leaves.

PhyB-Mediated Auxin Signaling is Required for the Systemic Enhancement of Photosynthetic Induction

Photoreceptors modify plant growth, development and stress responses via

alterations in phytohormone homeostasis (Jiao et al., 2007; Wang et al., 2016). Like polar auxin transport (PAT), light-induced signaling is basipetal in direction. We therefore examined how auxin accumulation was modified in the WT/WT, *phyA*/WT, *phyB1B2*/WT, and *cry1*/WT lines before and after the apex of the plants was exposed to WL. A pre-illumination with WL induced transcript levels of *FLAVIN MONOOXYGENASE (FZY)* in the apex and the accumulation of IAA in the apex and the 4th leaves (Fig. 2, A-C). *FZY* encodes flavin monooxygenase (FZY), a critical enzyme involved in a rate limiting step of IAA biosynthesis (Tivendale et al., 2010). Similar increases were also found in the apex and the 4th leaves of the *phyA*/WT and *cry1*/WT plants. In contrast, WL failed to increase *FZY* transcripts or IAA accumulation in either the apex or the 4th leaves of the *phyB1B2*/WT plants. Similar to increased IAA accumulation, WL induced an accumulation of *IAA15* transcripts, a marker of IAA signaling (Wei et al., 2012) and *PIN1* transcripts, a marker for PAT (Geldner et al., 2001; Ivanchenko et al., 2015) by 3-5 fold in the systemic leaves of the WT/WT, *phyA*/WT and *cry1*/WT plants, but not in the rootstock leaves of the *phyB1B2*/WT plants (Fig. 2D; Supplemental Fig. S5). Taken together, these results indicate that phyB was responsible not only for the observed increases in IAA biosynthesis in the apex but also for auxin signaling at the levels of the systemic leaves.

To explore the role of increased IAA accumulation on the systemic enhancement of photosynthetic induction, we applied IAA and *N*-1-naphthylphthalamicacid (NPA, an inhibitor for PAT) to the shoot apex either in the dark conditions or just prior to the pre-illumination treatment. Similar to the pre-illumination treatment, the application of IAA accelerated the induction of CO_2 assimilation in the systemic leaves. However, the application of NPA abolished the WL-induced enhancement of photosynthetic induction in the systemic leaves (Fig. 3, A and B; Supplemental Fig. S6). Therefore, we concluded that IAA synthesized in the apex may function as a systemic signal to influence the rate of induction of CO_2 assimilation in the distal leaves. To confirm this hypothesis, we grafted shoots with two leaves of WT and cyclophilin A *DIAGEOTROPICA* (*dgt*) mutant plants, which are auxin resistant, onto the stem at the 4th leaf position of either WT or *dgt* rootstocks, respectively. In this way, we were able to examine how the induction of CO_2 assimilation in the 4th leaf was altered by changes in the auxin signal arising in the apex. As predicted, WL pre-illumination-induced enhancement of the induction of CO_2 assimilation was

abolished in the WT leaves of the *dgt*/WT plants and in the *dgt* leaves of WT/*dgt* plants. Moreover, the T50 and T90 values were not changed by the pre-illumination (Fig. 3, C and D; Supplemental Fig. S7). Taken together, these results indicate that auxin signaling is essential for the pre-illumination-induced enhancement of the induction of CO_2 assimilation in systemic leaves.

Auxin-Triggered H_2O_2 Accumulation leads to Systemic Increases in the Induction of Photosynthesis by Activating Cyclic Electron Flow

Reactive oxygen species (ROS), such as H_2O_2 that are produced in the apoplast, can function as secondary messengers in hormone signaling pathways that underpin plant development and stress responses (Xia et al., 2015). In these studies, pre-illumination of the apex triggered an accumulation of transcripts encoding the RESPIRATORY BURST OXIDASE HOMOLOG 1 (RBOH1), together with an accumulation of H_2O_2 in the systemic leaves of the WT/WT, *phyA*/WT and *cry1*/WT plants, but not in the rootstock leaves of the *phyB1B2*/WT plants (Fig. 4, A and B). Similarly, H_2O_2 accumulation was observed in the walls of the mesophyll cells of 4th leaf of WT/WT plants, particularly those facing the intercellular spaces (Fig. 4E). However, the light-induced increases in *RBOH1* transcript levels and apoplastic H_2O_2 accumulation were abolished in the systemic leaves of *dgt*/WT plants and WT/*dgt* plants (Fig. 4, C-E). These results suggest that illumination of the apex resulted in apoplastic H_2O_2 accumulation in the systemic leaves, and that this process was dependent on auxin signaling.

To determine the role of *RBOH1* in pre-illumination dependent enhancement of photosynthetic induction in the systemic leaves, we generated *RBOH1*-RNAi plants (*rboh1*) and grafted portions onto WT plants (WT/*rboh1*). The 4th leaves of the *rboh1* plants with WT as scion had ca. 50% of the *RBOH1* transcripts as compared with that in WT/WT leaves (Supplemental Fig. S8). Significantly, the pre-illumination-induced enhancement of photosynthetic induction was compromised in the systemic *rboh1* leaves of WT/*rboh1* and *rboh1*/*rboh1* plants (Fig. 5, A-C; Supplemental Fig. S9A). Taken together, these results indicate that auxin-induced H_2O_2 production in the systemic leaves plays a critical role in the pre-illumination-associated enhancement of the induction of CO_2 assimilation.

CEF around PSI is particularly important in the induction phase of photosynthesis because it generates ATP at a time when non-cyclic electron flow is limited by the

availability of NADP (Joet et al., 2002; Joliot and Joliot, 2002). We compared rates of CEF in the systemic leaves of the WT/WT, WT/*rboh1* and *rboh1*/*rboh1* plants. The pre-illumination treatment of the apex significantly increased rates of CEF in the leaves of the WT/WT plants. This increase was not observed in the systemic leaves of WT/*rboh1* or *rboh1*/*rboh1* plants (Fig. 5, D-F; Supplemental Fig. S9, B and C). No enhancement of the rates of CEF was observed in the systemic leaves of *phyB1B2*/WT plants or *dgt*/WT plants (Fig. 6). However, increased CEF rates were observed in the systemic leaves of the *phyA*/WT and *cry1*/WT plants. These observations demonstrate that pre-illumination of the apex enhanced rates of CEF in a H_2O_2 –dependent manner and that this was linked to the activity of the *RBOH1* NADPH oxidase in the systemic leaves.

CEF-dependent ATP production is particularly important during the induction phase of photosynthesis because it drives electron transport and associated CO_2 assimilation when the electron acceptor NADP is in short supply (Foyer et al., 2012). An increase in the ATP content of 47.2%~57.7% was observed in the systemic WT leaves of the WT/WT, *phyA*/WT and *cry1*/WT plants after the apex had been illuminated with WL for 30 min. The top lighting-induced increase in ATP production was not found in the WT leaves of the *phyB1B2*/WT and *dgt*/WT plants (Fig. 7, A and B). Furthermore, ATP levels were not increased in the *rboh1* leaves after the pre-illumination treatment in the WT/*rboh1* plants (Fig. 7 C).

Systemic Effects on Photosynthetic Induction are Dependent on Cyclic Electron Flow in the Systemic Leaves

We next analyzed whether the increase in CEF is essential for the light-induced effects on photosynthetic induction in distal leaves. The *ORR* gene, which encodes a NAD(P)H dehydrogenase, was previously shown to be involved in the regulation of CEF in tomato (Nashilevitz et al., 2013). Virus-induced silencing of *ORR* (pTRV-*ORR*) resulted in a decrease in *ORR* transcript levels of 68.7% compared to the empty vector plants (pTRV). Under high light, the pTRV-*ORR* plants showed very low CEF rates (Supplemental Fig. S10). Moreover, the pTRV-*ORR* plants showed no response to apical pre-illumination in term of effects on the induction of CO_2 assimilation and CEF (Fig.8, A-D). While apical pre-illumination induced H_2O_2 accumulation in the systemic leaves of both pTRV and pTRV-*ORR* plants (Fig. 8E), there was no increase in ATP levels in the pTRV-*ORR* plants (Fig. 8F).

DISCUSSION

Rapid induction of photosynthesis in response to dark to light transitions and sharp increases in irradiance is critical to the survival of understory plants and gives a competitive advantage to plants within dense canopies. To date, studies on the induction of photosynthesis have been focused largely on responses in single leaves with scant attention to the systemic integration of the leaf network within the plant. The results presented here demonstrate that phyB-mediated IAA synthesis in the shoot apex leads to systemic signaling and to H_2O_2 accumulation in distal leaves. The subsequent increase in oxidation in the distal leaves activates CEF and ATP production, leading to a more rapid induction of CO_2 assimilation (Fig. 9). This systemic response is likely linked to enhanced light use efficiency in a fluctuating light environment. Systemic signaling following the perception of light by the apex, which is the uppermost organ in the shoot, provides the distal leaves with a preemptive advantage in terms of activation of photosynthesis and hence the ability to maximize carbon gain

The Apex-Induced Effects on the Induction of CO_2 Assimilation Are Phytochrome-Dependent

Light drives photosynthetic electron transport, light quality and quantity affecting photosynthesis in different ways to optimize growth. The results presented here demonstrate that pre-illumination of the apex with WL and with R light results in a more rapid induction of photosynthesis in distal leaves (Fig. 1, A-D). This effect on photosynthetic induction is directional and was observed only after exposure of the apex to WL or R light. This finding indicates that systemic signals originating from the young leaves at the apex, where cell division is rapid, are transduced to leaves in order to cause more rapid induction of photosynthesis. These observations are in agreement with an earlier observation that light-induced effects on photosynthesis are directional and that light perceived by mature leaves has little systemic effect on developing leaves in terms of the remodelling of photosynthesis (Murakami et al., 2014; Hou et al., 2015). The apex is likely to receive light signals earlier in the day than other parts of the plant. Thus, the transmission of light signals perceived at the apex to facilitate a more rapid photosynthetic induction in distal leaves probably evolved as a survival mechanism in understory plants in order to give a competitive

advantage within dense canopies.

The rate of photosynthetic induction of distal leaves was modified by the quality of light perceived at the apex by photoreceptors present in the apex. R light and FR light had positive and negative effects, respectively, on the speed of photosynthetic induction (Fig. 1C). Interestingly, R light-induced photosynthetic induction could be abolished by FR (Fig. 1E), suggesting that R and FR light-induced changes in photosynthetic induction is a photochromes-dependent response. In agreement with this, grafting experiments using *phyA* and *phyB* mutants as the scion revealed that CO_2 assimilation was induced more rapidly upon light perception by the apex in *phyA*/WT plants but not in the *phyB1B2*/WT combination (Fig. 1 F; Supplemental Fig. S4). These findings suggest that phyB plays a key role in the systemic effects on the induction of photosynthesis. In agreement with these observations, *phyB* mutants show decreased CO_2 assimilation rates (Hernan et al., 2009) and conversely overexpression of *PHYB* increased CO_2 assimilation rates compared to WT plants (Schittenhelm et al., 2004). Taken together, these results demonstrate that red light received by phyB at the shoot apex is the initial trigger for the systemic signaling to the distal leaves.

Auxin Synthesized in the Apex Functions as a Systemic Signal Leading to Effects on the Induction of CO_2 Assimilation

Phytochrome signaling mediates many systemic responses in plants including flowering time, tuberization and nodule development, processes which are regulated by light-induced changes in phytohormone homeostasis (Wit et al., 2016). Like auxin polar transport, the light-induced signaling pathway that influences photosynthetic induction is basipetal. Here we provide multiple lines of evidence showing that auxin is required for the systemic effects on the induction of photosynthesis. Firstly, WL and R light both induced an increase in *FZY* transcript levels in the apex, as well as IAA accumulation in the apex and an accumulation of *IAA15* transcripts, an auxin signaling marker in the distal leaves (Fig. 2). Secondly, the transmission of light-induced signals from the apex that mediate systemic increases in the induction of CO_2 assimilation was compromised in the WT leaves linked to a *phyB1B2* scion (Fig. 1 F; Supplemental Fig. S4). Thirdly, the application of IAA stimulated a more rapid induction of CO_2 assimilation. Conversely the application of an inhibitor of polar auxin transport compromised light-induced signal transmission to distal leaves (Fig. 3,

A and B; Supplemental Fig. S6). Fourthly, the transmission of light signals that enhance the induction of CO_2 assimilation in systemic leaves was abolished when an auxin resistant *dgt* mutant was used as the scion or rootstock (Fig. 3, C and D; Supplemental Fig. S7, A and B). While we cannot rule out the potential involvement of light-induced carbohydrate accumulation and transport from the apex, the apex and the youngest leaves are defined as "sink" tissues that have a net import of carbohydrate to drive metabolism, growth and development. These tissues are not generally considered to be "source", organs that export carbohydrate. Moreover, photosynthetic induction in distal leaves can only be observed after exposure to light intensities at PPFD levels to values higher than the light compensation point (Hou et al., 2015; Supplemental Fig. S2). We were unable to measure CO_2 assimilation rates in apex leaves due to their small size. However, CO_2 assimilation rates were very low in the developing leaves below the apex in the phyB plants, relative to the WT plants (Supplemental Fig. S11). Soluble carbohydrates can negatively regulate auxin biosynthesis via PHYTOCHROME-INTERACTING FACTOR (PIF) proteins, since PIFs negatively regulate phyB (Leivar et al., 2008; Sairanen et al., 2012). It is, therefore, possible that phyB functions as an integrator for light and sugar signaling in relation to auxin biosynthesis. To date, studies on the light regulation of auxin synthesis and polar auxin transport have produced contradictory results. For example, several studies have shown that exposure to low R/FR light ratios results in increased IAA accumulation and polar auxin transport in the hypocotyl (Tao et al., 2008; Keuskamp et al., 2010). However, such results have largely been obtained on very young Arabidopsis seedlings grown under conditions of minimal transpiration and photosynthesis, as occurs when plants are grown in closed Petri dishes, or on liquid media often containing sucrose, etc. (Tao et al., 2008; Keuskamp et al., 2010). Other studies have shown that low fluxes of red light enhance IAA synthesis and polar transport. The *phyB* mutant has decreased IAA accumulation in the stem in intact tomato plants (Liu et al., 2011). However, while plants grown under constant environmental conditions showed increased IAA accumulation during the night, plants grown in the field had increased IAA accumulation in the day (Lopez-Carbonell et al., 1992). Surprisingly, no studies have investigated the direct effects of light on auxin synthesis in apex even though auxin is thought to be mainly synthesized in the apex. Light- and phyB-mediated effects on IAA synthesis vary with between organs and environments (Ballaré, 2014; Krishna and Finlayson, 2014).

Plants may have developed these responses in auxin signaling as adaptation strategies to steep fluctuations in the light environment.

Auxin-Triggered H_2O_2 Production Acts as a Signal that Induces CEF and ATP Production in Systemic Leaves

Chloroplasts are a hub of redox control, which exerts a strong influence over gene expression, carbon assimilation and starch synthesis (Fey et al., 2005; Pfannschmidt et al., 2009). Phytohormones such as brassinosteroids (BRs) enhance CO_2 assimilation rates in a RBOH-dependent manner in plants (Jiang et al., 2012). Moreover, H_2O_2 activates CEF around PSI, in order to increase CO_2 assimilation (Strand et al., 2015). Auxin and BRs have overlapping functions in relation to the control of gene expression. Auxin also induces RBOH NADPH oxidase-dependent H_2O_2 production (Ivanchenko et al., 2013; Peer et al., 2013). In the present study, increased IAA accumulation and auxin signaling arising in the apex were shown to result in increased levels of *RBOH1* transcripts and in H_2O_2 accumulation in systemic leaves leading to increased CEF-dependent ATP production (Figs. 4-7). Crucially, blocking the auxin signal with a *dgt* scion or mutation of *RBOH1* genes in the systemic leaves abolished the signal-induced CEF and ATP accumulation in the systemic leaves (Figs.5-7). Taken together, these results demonstrate that CEF can be regulated in distal leaves by the auxin-dependent H_2O_2 production.

Non cyclic electron transport and cyclic electron flow around PSI are used to generate a proton gradient across the thylakoid membrane, a process that is coupled with ATP production (Shikanai, 2007; Foyer et al., 2012). Cyclic electron flow around PSI in higher plants consists of at least two partially redundant pathways known as the ferredoxinquinone oxidoreductase (FQR)- and NAD(P)H dehydrogenase NDH)-dependent pathways (Miyake, 2010). NDH complex deficiency in *orr* mutant tomato plants was defective in CEF (Nashilevitz et al., 2013). H_2O_2-induced CEF was therefore not observed in mutants deficient in NDH. In the present studies, suppression of NDH transcript using VIGS compromised the induction of CEF by systemic signals. These results show that the systemic effects on the induction of photosynthesis are linked to regulation of NDH-dependent CEF (Fig. 8).

Switching between cyclic and non-cyclic pathways provides flexibility in the ratios of ATP and NAPDH produced by the electron transport chain. The ratios of ATP to NAPDH production can therefore be adjusted to meet the needs of varying rates of

Benson–Calvin cycle activity, photorespiration and other metabolic pathways (Noctor and Foyer, 1999; Foyer et al., 2012). Thus flexibility also allows rapid responses to fluctuations in the light environment (Foyer and Harbinson, 1992; Foyer et al., 2012) In this regard, the systemic regulation of CEF may play a critical role in minimizing pseudocyclic electron flow and promoting the activation states of enzymes involved in CO_2 fixation, such as Rubisco activase (RCA) and fructose-1, 6-bisphosphatase (FBPase), which are modulated by the chloroplast redox status and ADP/ATP ratios, in the photosynthetic induction in response to irradiance.

The data presented here provide new insights into the regulation of photosynthesis. Evidence is presented showing that systemic regulation of the induction of photosynthesis in distal leaves is mediated by perception of red light at the apex via a phyB-associated pathway that promotes IAA biosynthesis and polar auxin transport, as illustrated in Fig 9. As a result, *RBOH1*-dependent H_2O_2 production in the systemic leaves induces cyclic electron flow in the chloroplasts and associated ATP production. These systemic and local signaling processes accelerate the rate of induction of CO_2 assimilation in systemic leaves. This study provides a mechanism by which plants can increase carbon gain in lower leaves in changing light environments via systemic regulation. Such mechanisms are likely to be very important in increasing light utilization efficiency in canopies for example at dawn, or in understory leaves where the light available in sunflecks must be used to maximize advantage in driving carbon gain.

MATERIALS AND METHODS

Plant Material and Growth Conditions

Wild-type tomato (*Solanum lycopersicum* L. cv. Ailsa Craig, cv. Moneymaker), cyclophilin A *DIAGEOTROPICA* (*dgt*) mutant in the Ailsa Craig background, and *phyA, phyB1B2* and *cry1* mutants in the Moneymaker background were used unless otherwise stated. Seedlings were grown in pots with a mixture of 3 parts peat to 1 part vermiculite, receiving Hoagland's nutrient solution. The growth conditions were as follows: 12 h photoperiod, temperature of 25/20 ^{o}C (day/night), and photosynthetic photo flux density (PPFD) of 600 μmol m^{-2} s^{-1}.

To generate the *RBOH1* RNAi construct, a 318-bp specific DNA fragment of *SlRBOH1* was PCR-amplified with the specific primers *SlRBOH1*-F (5′-GGCCatttaaatggatccCGTTCAGCTCTCATTACC-3′) and *SlRBOH1*-R

(5′-TTggcgcgcctctagaCCGAAGATAGATGTGTGT-3′), which had been tailed with *BamHI*/*Xba*I and *Swa*I/*Asc*I restriction sites at the 5′ end, respectively. Then, the amplified products were digested with *BamHI*/*Xba*I and *Swa*I/*Asc*I and ligated into the pFGC5941 vector at the *BamHI*/*Xba*I restriction site in the sense orientation and at the *Swa*I/*Asc*I restriction site in the antisense orientation. The resulting plasmid was transformed into *Agrobacterium tumefaciens* strain EHA105 and transformed into tomato cotyledons of Ailsa Craig as described by Fillatti et al (1987). Transgenic plants were identified for resistance to Basta and then by qRT-PCR analysis.

To determine the role of cyclic electron flux in pre-illumination-induced CO_2 assimilation, we used virus-induced gene silencing (VIGS) to suppress the transcript of *Orange Ripening* (*ORR,* Nashilevitz et al., 2013) with the tobacco rattle virus (TRV)-based vectors (pTRV1/2) (Liu et al., 2002). The *ORR* cDNA fragment was PCR-amplified using as the forward primer CGgaattcGATCCCGAAACCTTTGCTT and the reverse primer CCGctcgagTCCATTGTAATTGAACCCA'. The amplified *ORR* fragment was digested with *Eco*RI and *Xho*I, and ligated into *the* corresponding sites of the pTRV2 vector. Empty pTRV2 vector was used as a control. All constructs were confirmed by sequencing and subsequently transformed into *Agrobacterium tumefaciens* strain GV3101. VIGS was performed by infiltration into the fully expanded cotyledons of 15-d-old tomato seedlings with *A. tumefaciens* harboring a mixture of pTRV1 and pTRV2-target gene in a 1:1 ratio. Plants were grown at 21 ^{o}C in a growth chamber with a 12 h day length for 30 d until control pTRV-*PDS* plants (silencing of the gene encoding phytoene desaturase) showed strong bleaching (Ekengren et al., 2003). qRT-PCR was performed to determine the gene silencing efficiency (Livak and Schmittgen, 2001).

To determine the role of photoreceptors in photosynthetic induction, shoots of wild type (WT), *phyA*, *phyB1B2* and *cry1* plants with two developing leaves at 3~4 cm in length was grafted onto 4th leaf stem of WT plants, resulting in four groups of seedlings designated as WT/WT, *phyA*/WT, *phyB1B2*/WT and *cry1*/WT according to the scions, respectively. In the same way, we grafted shoots with two leaves of *dgt* mutant plants, which is auxin resistant onto stem of WT plants (*dgt* /WT), WT shoots onto stem of *dgt* plants (WT/ *dgt*) or onto that of *RBOH1*-RNAi plants (WT/*rboh1*), shoots of *RBOH1*-RNAi plants onto *RBOH1*-RNAi plants (*rboh1*/*rboh1*) . The grafted plants were transferred to growth chambers with the following environmental conditions: 12-h photoperiod, temperature of 25/20 °C (day/night) and photosynthetic

photon flux density (PPFD) of 600 μmol m^{-2} s^{-1}.

Experimental Design and Treatments

Leaves in a plant were marked from No. 1 to No. 6 from cotyledons. Six independent experiments were carried out. In experiment 1, the 1-3th leaves, the 5-6th leaves and the apex were illuminated with white light (Philips, The Netherlands) at 50, 150 and 300 μmol m^{-2} s^{-1} for 30 minutes before the photosynthetic inductions of the 4th leaves were measured afterwards (Supplemental Fig. S1). In experiment 2, the apex of WT plants at 6-leaf stage was illuminated with red (R, 660 nm) or far-red (FR, 735 nm) at 300 μmol m^{-2} s^{-1} for 30 minutes or light with R/FR ratio at 2:1, 1:1 and 1:2, respectively, in which R light intensity was kept at 300 μmol m^{-2} s^{-1}. Meanwhile, reciprocal R /FR light pulse at 5 min interval, which lasted 60 min with 6 cycles, was applied onto the apex for testing the reversibility of the positive effect of R light on the photosynthetic induction. Mono-spectrum light was supplied with light-emitting diode (LED) source (Philips, The Netherlands). In other experiments, the apex of WT/WT, *phyA*/WT, *phyB1B2*/WT, and *cry1*/WT (Experiment 3), *dgt*/WT and WT/*dgt* (Experiment 4), WT/*rboh1* and *rboh1*/*rboh1* (Experiment 5), pTRV and pTRV-*ORR* plants (Experiment 6) at 6-leaf stage was pre-illuminated with WL at 300 μmol m^{-2} s^{-1} for 30 minutes before the photosynthetic inductions of the 4th leaves were measured afterwards. To study the role of IAA in the photosynthetic induction, IAA at 10 μM and *N*-1-naphthylphthalamicacid (NPA) at 10 μM were applied onto apex 30 min before gas exchange in the 4th leaves was determined. In all cases, plant without pre-illumination of apex (dark) was used as control.

Gas Exchange and Chl Fluorescence

Gas exchange measurements were performed using a LI-6400 Portable Photosynthesis System (LI-6400; LI-COR, Lincoln, NE, USA). The CO_2 concentration (400 μmol mol^{-1}), air humidity (60%), PPFD (1500 μmol m^{-2} s^{-1}) and leaf temperature (25 °C) were controlled by an automatic control device of the instrument. The photosynthetic rate (Pn) was recorded every 20 s. Four plants were used in each measurement.

Chlorophyll (Chl) fluorescence was performed using a Dual-PAM 100 Chl fluorescence analyzer (Heinz Walz, Effeltrich, Germany) as described in Eiji et al., (2010). For the determination of chlorophyll fluorescence, plants were adapted in the

dark for 30min prior to measurement. After 4 min, the actinic light (AL; 250 μmol m^{-2} s^{-1}) was turned off and fluorescence yield changes were continuously recorded (Yang et al., 2007). Four plants were used for each replicate. Relative Chl fluorescence, expressed as the rake ratio of the induction curve, was calculated from the one time regression equation y=a+bx, where y, a and x are the fluorescence yield, the rake ratio of the induction curve and time duration, respectively, during the fluorescence rise.

Measurement of IAA Levels

IAA extraction and quantification were performed using previously reported procedures with minor modifications (Durgbanshi et al., 2005; Wu et al., 2007; Boelaert et al., 2013). Briefly, 100 mg of frozen leaf material was homogenized in 1 mL of ethyl acetate which had been spiked with D_5-IAA (C/D/N Isotopes Inc, Canada) as internal standards with a final concentration of 100 ng mL^{-1}. Tubes were centrifuged at 18,000 *g* for 10 min at 4 °C. The pellet was re-extracted with 1 mL of ethyl acetate. Both supernatants were evaporated to dryness under N_2. The residue was re-suspended in 0.5 mL of 70% methanol (v/v), centrifuged, and the supernatants were then analyzed in a liquid chromatography tandem mass spectrometry system (Varian 320-MS LC/MS, Agilent Technologies, Amstelveen, the Netherlands). The parent ions, daughter ions, and collision energies used in these analyses are listed in Supplemental Table S2.

H_2O_2 Quantification, Histochemical Analysis, and Cytochemical Detection

H_2O_2 was extracted from leaf tissue and measured as described in our earlier study (Xia et al., 2009). H_2O_2 was also visualized at the subcellular level using $CeCl_3$ for localization, as described previously (Zhou et al., 2012). The sections were examined using a transmission electron microscope (H7650; Hitachi, Tokyo, Japan) at an accelerating voltage of 75 kV to detect the electron-dense $CeCl_3$ deposits that were formed in the presence of H_2O_2.

qRT-PCR Analysis

Total RNA was extracted from tomato leaves using RNAprep Pure Plant Kit (Tiangen Biotech Co., Ltd, Beijing, China) according to the supplier's recommendation. Residual DNA was removed with RNase Mini Kit (Qiagen, Germany). One microgram of total RNA was reverse transcribed using a ReverTra

Ace qPCR RT Kit (Toyobo, Osaka, Japan), following the supplier's recommendation. On the basis of EST sequences, the gene-specific primers are shown in Supplemental Table S2 and used for amplification. qRT-PCR was performed using a Roche LightCycler 480 real-time PCR machine (Roche, Switzerland). The PCR reaction was run for 95 °C for 3 min, followed by 40 cycles of 30 s at 95 °C, 30 s at 58 °C and 1 min at 72 °C. The tomato *Actin* was used as an internal control. The relative gene expression was calculated as previously described (Livak and Schmittgen, 2001).

Determination of ATP Content

To determine ATP content in leaves, 0.1 g leaf samples was immediately placed in tubes containing 2 mL Tris–HCl (pH 7.8). The tubes with samples were then kept for 10 min at 100 °C in a boiling water bath for ATP extraction. One hundred μL of ATP extraction solution was used for analysis after sample cooling at room temperature. The detailed procedures were performed following the instructions in the ATPlite 1step Assay System (Perkin Elmer, Waltham, USA).

LITERATURE CITED

Allen JF (2003) Cyclic, pseudocyclic and noncyclic photophosphorylation: new links in the chain. Trends Plant Sci **8:** 15–19

Araya T, Noguchi KO, Terashima I (2008) Manipulation of light and CO_2 environments of the primary leaves of bean (*Phaseolus vulgaris* L.) affects photosynthesis in both the primary and the first trifoliate leaves: involvement of systemic regulation. Plant Cell Environ **31:** 50-61

Bai KD, Liao DB, Jiang DB, Cao KF (2008) Photosynthetic induction in leaves of co-occurring *Fagus lucida* and *Castanopsis lamontii* saplings grown in contrasting light environments. Trees **22:** 449-462

Boelaert J, Lynen F, Glorieux G, Eloot S, Landschoot MV, Waterloos MA, Sandra P, Vanholder R (2013) A novel UPLC-MS-MS method for simultaneous determination of seven uremic retention toxins with cardiovascular relevance in chronic kidney disease patients. Anal Bioanal Chem **405:** 1937-1947

Ballaré CL (2014) Light regulation of plant defense. Annu Rev Plant Biol **65:** 335-363

Bidwell RG, Turner WB (1966) Effect of growth regulators on CO_2 assimilation in leaves, and its correlation with the bud break response in photosynthesis. Plant Physiol **41:** 267-270

Casson SA, Hetherington AM (2014) phytochrome B is required for light-mediated systemic control of stomatal development. Curr Biol **24:** 1216-1221

Coupe SA, Palmer BG, Lake JA, Overy SA, Oxborough K, Woodward FI, Gray JE, Quick WP (2006) Systemic signaling of environmental cues in Arabidopsis leaves. J Exp Bot **57:** 329-341

Durgbanshi A, Arbona V, Pozo O, Miersch O, Sancho JV, Gómez-Cadenas A (2005) Simultaneous determination of multiple phytohormones in plant extracts by liquid chromatography-electrospray tandem mass spectrometry. J Agri Food Chem **53:** 8437-8442

Eiji G, Yoshichika K, Michito T (2010) The post-illumination chlorophyll fluorescence transient indicates the RuBP regeneration limitation of photosynthesis in low light in Arabidopsis. Febs Lett **584:** 3061-3064

Ekengren SK, Liu Y, Schiff M, Dinesh-Kumar SP, Martin GB (2003) Two MAPK cascades, NPR1, and TGA transcription factors play a role in Pto-mediated

disease resistance in tomato. Plant J **36:** 905-917

Fey V, Wagner R, Bräutigam K, Pfannschmidt T (2005) Photosynthetic redox control of nuclear gene expression. J Exp Bot **56:** 1491-1498

Fillatti JAJ, Kiser J, Rose R, Comai L (1987) Efficient transfer of a glyphosate tolerance gene into tomato using a binary *Agrobacterium tumefaciens* vector. Nat Biotech **5:** 726-730

Foyer CH, Harbinson J (1992) Control of the quantum efficiencies of photosystems I and II, electron flow, and enzyme activation following dark-to-light transitions in pea leaves. Plant Physiol **99:** 979-986

Foyer CH, Neukermans J, Queval G, Noctor G, Harbinson J (2012) Photosynthetic control of electron transport and the regulation of gene expression. J Exp Bot **63:** 1637-1661

Geldner N, Friml J, Stierhof YD, Jürgens G, Palme K (2001) Auxin transport inhibitors block PIN1 cycling and vesicle trafficking. Nature **413:** 425-428

Halliday KJ, Martínez-García JF, Josse EM (2009) Integration of light and auxin signaling. Cold Spring Harb Perspect Biol **1:** a001586

Hauser BA, CordonnierPratt MM, DanielVedele F, Pratt LH (1995) The phytochrome gene family in tomato includes a novel subfamily. Plant Mol Biol **29**: 1143-1155

Hayat Q, Hayat S, Ali B, Aqil A (2009) Auxin analogues and nitrogen metabolism, photosynthesis, and yield of chickpea. J Plant Nutr **32:** 1469-1485

Hernan EB, Matias LR, Javier EM, Edmundo LP, Laura S, Marcelo JY, Jorge JC (2009) Phytochrome B enhances photosynthesis at the expense of water-use efficiency in Arabidopsis. Plant Physiol **150:** 1083-1092

Hou F, Jin LQ, Zhang ZS, Gao HY (2015) Systemic signalling in photosynthetic induction of *Rumex* K-1 (*Rumex patientia* × *Rumex tianschaious*) leaves. Plant Cell Environ **38:** 685-692

Husaineid SSH, Kok RA, Schreuder MEL, Hanumappa M, Cordonnier-Pratt MM, Pratt LH, van der Plas LHW, van der Krol AR (2007) Overexpression of homologous phytochrome genes in tomato: exploring the limits in photoperception. J Exp Bot 58: 615-626

Ivanchenko MG, Os DD, Monshausen GB, Dubrovsky JG, Bednářová A, Krishnan N (2013) Auxin increases the hydrogen peroxide (H_2O_2) concentration in tomato (*Solanum lycopersicum*) root tips while inhibiting root growth. Ann Bot

112: 1107-1116

Ivanchenko MG, Zhu JS, Wang BJ, Medvecka E, Du YL, Azzarello E, Mancuso S, Megraw M, Filichkin S, Dubrovsky JG, Friml J, Geisler M (2015) The cyclophilin A DIAGEOTROPICA gene affects auxin transport in both root and shoot to control lateral root formation. Development **142:** 712-721

Jiang YP, Cheng F, Zhou YH, Xia XJ, Mao WH, Shi K, Chen Z, Yu JQ (2012) Cellular glutathione redox homeostasis plays an important role in the brassinosteroid-induced increase in CO_2 assimilation in *Cucumis sativus*. New Phytol **194:** 932–943

Jiao Y, Lau OS, Deng XW (2007) Light-regulated transcriptional networks in higher plants. Nat Rev Genet **8:** 217-230

Joet T, Cournac L, Peltier G, Havaux M (2002) Cyclic electron flow around photosystem I in C-3 plants. In vivo control by the redox state of chloroplasts and involvement of the NADH-dehydrogenase complex. Plant Physiol **128:** 760-769

Joliot P, Joliot A (2002) Cyclic electron transfer in plant leaf. Proc Natl Acad Sci USA **99:** 10209-10214

Keuskamp DH, Stephan P, Voesenek LACJ, Peeters AJM, Ronald P (2010) Auxin transport through PIN-FORMED 3 (PIN3) controls shade avoidance and fitness during competition. Proc Natl Acad Sci USA **107:** 22740-22744

Krishna RS, Finlayson SA (2014) Phytochrome B promotes branching in Arabidopsis by suppressing auxin signaling. Plant Physiol **164:** 1542-1550

Lake JA, Woodward FI, Quick WP (2002) Long-distance CO_2 signalling in plants. J Exp Bot **53:** 183-193

Leakey ADB, Press MC, Scholes JD (2003) Patterns of dynamic irradiance affect the photosynthetic capacity and growth of dipterocarp tree seedlings. Oecologia **135:** 184-193

Leakey ADB, Scholes JD, Press MC (2005) Physiological and ecological significance of sunflecks for dipterocarp seedlings. J Exp Bot **56:** 469-482

Leivar P, Monte E, Al-Sady B, Carle C, Storer A, Alonso JM, Ecker JR, Quail, PH (2008) The Arabidopsis phytochrome-interacting factor PIF7, together with PIF3 and PIF4, regulatesresponses to prolonged red light by modulating phyB levels. Plant Cell **20**: 337-352.

Liu X, Cohen JD, Gardner G (2011) Low-fluence red light increases the transport and biosynthesis of auxin. Plant Physiol **157:** 891-904

Liu Y, Schiff M, Marathe R, Dinesh-Kumar SP (2002) Tobacco *Rar1*, *EDS1* and *NPR1/NIM1* like genes are required for *N*-mediated resistance to tobacco mosaic virus. Plant J **30:** 415-429

Livak KJ, Schmittgen TD (2001) Analysis of relative gene expression data using real-time quantitative PCR and the $2^{-\Delta\Delta C T}$ method. Methods **25:** 402-408

Ljung K, Bhalerao RP, Sandberg G (2001) Sites and homeostatic control of auxin biosynthesis in Arabidopsis during vegetative growth. Plant J **28:** 465-474

Lopez-Carbonell M, Alegre L, Prinsen E, Onckelen HV (1992) Diurnal fluctuations of endogenous IAA content in aralia leaves. Biol Plant **34:** 223-227

Mittler R, Blumwald E (2015) The roles of ROS and ABA in systemic acquired acclimation. Plant Cell **27:** 64-70

Miyake C (2010) Alternative electron flows (water-water cycle and cyclic electron flow around PSI) in photosynthesis: molecular mechanisms and physiological functions. Plant Cell Physiol **51:** 1951-1963

Montgomery RA, Givnish TJ (2008) Adaptive radiation of photosynthetic physiology in the Hawaiian lobeliads: dynamic photosynthetic responses. Oecologia **155:** 455-467

Murakami K, Matsuda R, Fujiwara K (2014) Light-induced systemic regulation of photosynthesis in primary and trifoliate leaves of *Phaseolus vulgaris*: effects of photosynthetic photon flux density (PPFD) versus spectrum. Plant Biol **16:** 16-21

Nashilevitz S, Melamed-Bessudo C, Izkovich Y, Rogachev I, Osorio S, Itkin M, Adato A, Pankratov I, Hirschberg J, Fernie AR (2013) An orange ripening mutant links plastid NAD(P)H dehydrogenase complex activity to central and specialized metabolism during tomato fruit maturation. Plant Cell **2013:** 1977-1997

Noctor G, Foyer CH (1999) A re-evaluation of the ATP: NADPH budget during C3 photosynthesis: a contribution from nitrate assimilation and its associated respiratory activity? J Exp Bot **49:** 1895-1908

Pearcy RW, Seemann JR (1990) Photosynthetic induction state of leaves in a soybean canopy in relation to light regulation of ribulose-1-5-bisphosphate carboxylase and stomatal conductance. Plant Physiol **94:** 628-633

Peng Q, Wang H, Tong J, Kabir MH, Huang Z, Xiao L (2013) Effects of indole-3-acetic acid and auxin transport inhibitor on auxin distribution and development of peanut at pegging stage. Sci Hort **162:** 76-81

Peer WA, Cheng Y, Murphy AS (2013) Evidence of oxidative attenuation of auxin signaling. J Exp Bot **64:** 2629-2639

Pfannschmidt T, Bräutigam K, Wagner R, Dietzel L, Schröter Y, Steiner S, Nykytenko A (2009) Potential regulation of gene expression in photosynthetic cells by redox and energy state: approaches towards better understanding. Ann Bot **103:** 599-607

Pieterse CMJ, Dicke M (2007) Plant interactions with microbes and insects: from molecular mechanisms to ecology. Trends Plant Sci 12: 564-569

Sairanen I, Novak O, Pencik A, Ikeda Y, Jones B, Sandberg G, Ljung K (2012) Soluble carbohydrates regulate auxin biosynthesis via PIF proteins in Arabidopsis Plant Cell **24**: 4907-4916

Schittenhelm S, Menge-Hartmann U, Oldenburg E (2004) Photosynthesis, carbohydrate metabolism, and yield of Phytochrome-B-overexpressing potatoes under different light regimes. Crop Sci **44:** 131-143

Shikanai T (2007) Cyclic electron transport around photosystem I: genetic approaches. Annu Rev Plant Biol **58:** 199-217

Strand DD, Livingston AK, Mio SC, Froehlich JE, Maurino VG, Kramer DM (2015) Activation of cyclic electron flow by hydrogen peroxide in vivo. Proc Natl Acad Sci USA **112:** 5539-5544

Tao Y, Ferrer JL, Ljung K, Pojer F, Hong F, Long JA, Li L, Moreno JE, Bowman ME, Ivans LJ (2008) Rapid synthesis of auxin via a new tryptophan-dependent pathway is required for shade avoidance in plants. Cell **133:** 164-176

Thorpe MR, Ferrieri AP, Herth MM, Ferrieri RA (2007) C-11-imaging: methyl jasmonate moves in both phloem and xylem, promotes transport of jasmonate, and of photoassimilate even after proton transport is decoupled. Planta **226:** 541-551

Tivendale ND, Davies NW, Molesworth PP, Davidson SE, Smith JA, Lowe EK, Reid JB, Ross JJ (2010) Reassessing the role of N-hydroxytryptamine in auxin biosynthesis. Plant Physiol **154:** 1957-1965

Turgeon R, Wolf S (2009) Phloem transport: cellular pathways and molecular trafficking. Annu Rev Plant Biol **60:** 207-221

Walker DA (1973) Photosynthetic induction phenomena and light activation of rubulose diphosphate carboxylase. New Phytol **72:** 209-235

Weller JL, Schreuder ME, Smith H, Koornneef M, Kendrick RE (2000)

Physiological interactions of phytochromes A, B1 and B2 in the control of development in tomato. Plant J **24**: 345-356.

Wang F, Guo ZX, Li HZ, Wang MM, Onac E, Zhou J, Xia XJ, Shi K, Yu JQ, Zhou YH (2016) Phytochrome A and B function antagonistically to regulate cold tolerance via abscisic acid-dependent jasmonate signaling. Plant Physiol **170:** 459-471

Wei D, Yang Y, Ren Z, Audran-Delalande C, Mila I, Wang X, Song H, Hu Y, Bouzayen M, Li Z (2012) The tomato *SlIAA15* is involved in trichome formation and axillary shoot development. New Phytol **194:** 379-390

Wit MD, Galvão VC, Fankhauser C (2016) Light-mediated hormonal regulation of plant growth and development. Annu Rev Plant Biol **67:** 513-537

Wu J, Hettenhausen C, Meldau S, Baldwin IT (2007) Herbivory rapidly activates MAPK signaling in attacked and unattacked leaf regions but not between leaves of *Nicotiana attenuata*. Plant Cell **19:** 1096-1122

Xia XJ, Wang YJ, Zhou YH, Tao Y, Mao WH, Shi K, Asami T, Chen Z, Yu JQ (2009) Reactive oxygen species are involved in brassinosteroid-induced stress tolerance in cucumber. Plant Physiol **150:** 801-814

Xia XJ, Zhou YH, Shi K, Zhou J, Foyer CH, Yu JQ (2015) Interplay between reactive oxygen species and hormones in the control of plant development and stress tolerance. J Exp Bot **66:** 2839-2856

Yamori W, Shikanai T, Makino A (2015) Photosystem I cyclic electron flow via chloroplast NADH dehydrogenase-like complex performs a physiological role for photosynthesis at low light. Sci Rep **5:** 13908

Yamori W, Shikanai T (2016) Physiological functions of cyclic electron transport around photosystem I in sustaining photosynthesis and plant growth. Annu Rev Plant Biol **67:**81-106

Yang Y, Yan CQ, Cao BH, Xu HX, Chen JP, Jiang DA (2007) Some photosynthetic responses to salinity resistance are transferred into the somatic hybrid descendants from the wild soybean *Glycine cyrtoloba* ACC547. Physiol Plant **129:** 658-669

Fu ZQ, Dong X (2013) Systemic acquired resistance: turning local infection into global defense. Annu Rev Plant Biol **64:** 839-863

Zhou J, Wang J, Shi K, Xia XJ, Zhou YH, Yu JQ (2012) Hydrogen peroxide is involved in the cold acclimation-induced chilling tolerance of tomato plants.

Plant Physiol Biochem **60:** 141-149

Zimmermann MR, Maischak H, Mithofer A, Boland W, Felle HH (2009) System potentials, a novel electrical long-distance apoplastic signal in plants, induced by wounding. Plant Physiol **149:** 1593-1600

Figure legends

Figure 1. The influence of systemic light signaling on the induction phase of net CO_2 assimilation (Pn; A, C-F) and the time required to reach 50% or 90% of the maximum Pn (T50 or T90) (B). In A and B, pre-illumination was provided to the shoot apex, upper leaves (UL, 5-6th leaves) and lower leaves (LL, 1st-3th) with white light (L) at an intensity of 300 μmol m^{-2} s^{-1} for 30 min before CO_2 assimilation was analyzed in the 4th leaves. In C, the apex was pre-illuminated with R or FR light for 30 min before CO_2 assimilation was analyzed in the 4th leaves. In D, the apex was pre-illuminated with different R/FR light ratios for 30 min, in which R light was kept at 300 μmol m^{-2} s^{-1}, before CO_2 assimilation was measured in the 4th leaves. In E, reciprocal R /FR light pulse at 5 min interval with 6 cycles, was applied onto the apex before CO_2 assimilation was measured in the 4th leaves. In F, pre-illumination was provided by white light at an intensity of 300 μmol m^{-2} s^{-1} for 30 min before CO_2 assimilation was analyzed in the 4th leaves of the grafted plants. During the illumination treatments, the other parts of the plant were kept in darkness. Net photosynthetic rates are expressed as percentage of the maximum Pn. Plants without pre-illumination (dark, D) were used as controls. L, white light; R, red light; FR, far red light. Values are the means of four plants ± SD. Different letters indicate significant differences at $P < 0.05$ according to Tukey's test.

Figure 2. The effects of pre-illumination of the apex on *FZY* and *IAA15* transcript levels and on the accumulation of IAA in grafted plants. A, *FZY* transcript levels in the apex. B, IAA accumulation in the apex. C, IAA accumulation and D, *IAA15* transcript levels in the 4th leaves. Samples were harvested at 30 min after the pre-illumination for A-D. Plants without pre-illumination (dark, D) were used as controls. L, white light; *phyA*/WT, plants with *phyA* mutants as scion; *phyB1B2*/WT, plants with *phyB1B2* mutants as scion; *cry1*/WT, plants with *cry1* mutants as scion. During the illumination treatments, the other parts of the plant were kept in darkness. Values are the means of four plants ± SD. Different letters indicate significant differences at $P < 0.05$ according to Tukey's test.

Figure 3. The rate of net CO_2 assimilation (Pn; A and C) during the induction phase of photosynthesis in 4th leaves and the time required to reach 50 or 90% of the maximum Pn (T50 or T90) (B and D). A and B, effects of IAA (10 μM) and NPA (10 μM) on the induction phase of CO_2 assimilation in the 4th leaves and the time required to reach T50 or T90. C and D, The induction of CO_2 assimilation in the 4th leaves and the time required to reach T50 or T90 of the grafted plants with *dgt* as scion or rootstock. D, Dark control; L, White light (300 μmol m^{-2} s^{-1}) applied to the apex for 30 min before the measurement of CO_2 assimilation and the harvest of samples. During the illumination treatments, the other parts of the plant were kept in darkness. Net photosynthesis rates are expressed as percentages of the maximum Pn. Values are the means of four plants ± SD. Different letters indicate significant differences at $P < 0.05$ according to Tukey's test.

Figure 4. The influence of scion genotypes and lighting onto apex on the levels of *RBOH1* transcripts and H_2O_2 accumulation in the systemic leaves. A, The influence of different photoreceptor mutants as scions on the levels of *RBOH1* transcripts in the systemic leaves of grafted plants. B, The influence of different photoreceptor mutants as scions on the accumulation of H_2O_2 in the systemic leaves of grafted plants. C, *RBOH1* transcripts in the systemic leaves in plants with *dgt* as scion or rootstock. D, Accumulation of H_2O_2 in the systemic leaves in grafted plants with *dgt* as scion or rootstock. E, Cytochemical localization of H_2O_2 accumulation in mesophyll cells of systemic leaves with $CeCl_3$ staining in grafted plants with *dgt* as scion or rootstock. The apex was exposed to white light (L) at 300 μmol m^{-2} s^{-1} for 30 min or not (D), then the 4th leaves (SL) of the grafted plants were harvested soon for the analysis and cytochemical detection of H_2O_2**.** During the illumination treatments, the other parts of the plant were kept in darkness. Values are the means of four plants ± SD with different letters indicating significant differences at $P < 0.05$ according to Tukey's test in A-D. Arrows in the electron microscopy pictures indicate, H_2O_2-induced $CeCl_3$ precipitates in the apoplast of systemic leaves in E.

Figure 5. The requirement for *RBOH1* in systemic light signaling from the shoot apex to distal leaves for the regulation of CO_2 assimilation rates and cyclic electron flow

(CEF) during the induction phase of photosynthesis. A-C, Time-course of increases in net photosynthesis rate (Pn) during photosynthetic induction and the time required to reach 50% or 90% of the maximum Pn (T50 or T90) in the 4th leaves. Net photosynthetic rates are expressed as percentages of the maximum Pn. D and E, Typical traces of Chl a fluorescence quenching after 4-min actinic illumination (AL; 250 μmol m^{-2} s^{-1}) in grafted plants with *rboh1* mutant rootstocks. F, Relative Chl fluorescence was expressed as the rake ratio of the induction curve. Irradiance to the shoot apex (Top lighting) was performed with white light (L) at 300 μmol m^{-2} s^{-1} for 30 min. Plants without pre-illumination (dark, D) were used as controls. During the illumination treatments, the other parts of the plant were kept in darkness. Values are the means of four plants ± SD. Different letters indicate significant differences at $P < 0.05$ according to Tukey's test.

Figure 6. The effect of *dgt* scions on the irradiance to the shoot apex-dependent changes in cyclic electron flow (CEF). A, Typical Chl a fluorescence quenching after 4-min actinic illumination (AL; 250 μmol m^{-2} s^{-1}) for grated plants with different photoreceptor mutants as scions. B, Typical trace of Chl a fluorescence quenching after 4-min actinic illumination (AL; 250 μmol m^{-2} s^{-1}) for plants with *dgt* mutant as scion. C, Relative Chl fluorescence was expressed as the rake ratio of the induction curve. Irradiance to the shoot apex (Top lighting) was performed with white light (L) at 300 μmol m^{-2} s^{-1} for 30 min. Plants without pre-illumination (dark, D) were used as controls. During the illumination treatments, the other parts of the plant were kept in darkness. Values are the means of four plants ± SD. Different letters indicate significant differences at $P < 0.05$ according to Tukey's test.

Figure 7. The influence of *phyA, phyB1B2* and *cry1* (A) and *dgt* (B) as scions in grafted plants, and *RBOH1* suppression in the leaves of the rootstock (C) on the effects of irradiance to the apex on ATP accumulation in the 4th leaves. D, Dark control. L, White light (300 μmol m^{-2} s^{-1}) was applied to the apex (top lighting) for 30 min. Plants without pre-illumination (dark, D) were used as controls. Samples were harvested after the whole plants were exposed to WL for 8 min with pre-illumination. During the illumination treatments, the other parts of the plant were kept in darkness. Values are the means of four plants ± SD. Different letters indicate significant differences at $P < 0.05$ according to Tukey's test.

Figure 8. The requirement for *ORR* in systemic light signaling effects on the induction phase of photosynthesis in distal tomato leaves, including the time course of increases in net photosynthetic rate (Pn) during photosynthetic induction, the time required to reach 50% or 90% of the maximum Pn, cyclic electron flow (CEF), H_2O_2 accumulation and ATP accumulation in the 4^{th} leaves. A and B, Time course of increases in Pn during photosynthetic induction and the time required to reach 50% or 90% of the maximum Pn (T50 or T90) in 4^{th} leaves. Net photosynthetic rates are expressed as percentages of the maximum Pn. C and D, the effect of *ORR* silencing on cyclic electron flow (CEF) in the 4^{th} leaves during photosynthetic induction. E, the effect of *ORR* on H_2O_2 accumulation in the 4^{th} leaves after pre-illumination of the apex with white light (L) at 300 μmol m^{-2} s^{-1} for 30 min. F, the effect of *ORR* on ATP accumulation in the 4^{th} leaves during photosynthetic induction. Samples were harvested after the whole plants were exposed to L for 8 min with pre-illumination. D, dark control. L, White light (300 μmol m^{-2} s^{-1}) was applied to the apex for 30 min before the measurement of CO_2 assimilation rates. During the illumination treatments, the other parts of the plant were kept in darkness. Values are the means of four plants ± SD. Different letters indicate significant differences at $P < 0.05$ according to Tukey's test.

Figure 9. A working model depicting how light perception at the apex initiates an auxin- and redox-dependent systemic signaling pathway leading to enhanced rates of photosynthetic induction in distal leaves. In this model, R perceived by phyB and FR perceived by phyA function antagonistically to regulate IAA biosynthesis. As a result of light-perception driven polar auxin transport (PAT), IAA triggers systemic H_2O_2 production in distal leaves which is able to accelerate cyclic electron flow (CEF) around PSI leading to increased ATP production. In this way, light perception by the apex can enhance photosynthetic CO_2 assimilation and resultant carbon gain in distal leaves.

Supplemental Data

The following supplemental materials are available.

Supplemental Figure S1. Sketch map of the plant materials and experiment design.

Supplemental Figure S2. Effects of pre-illumination at different white light intensity on the induction of photosynthesis in the systemic leaves.

Supplemental Figure S3. Effects of pre-illumination on the induction of photosynthesis in plants with *cry1* as scion.

Supplemental Figure S4. The influence of systemic light signaling on the time required to reach 50% or 90% of the maximum net photosynthetic rate (T50 or T90) in photosynthetic induction.

Supplemental Figure S5. Relative transcript of *PIN1* in the 4^{th} leaf as influenced by the pre-illumination.

Supplemental Figure S6. Effects of application of NPA on the induction of photosynthesis.

Supplemental Figure S7. Effects of pre-illumination on the induction of photosynthesis in the 4^{th} leaf in grafting plants with *dgt* as rootstock.

Supplemental Figure S8. Relative transcript of *RBOH1* in the scion leaves and rootstock leaves in grafted plants used for the experiment (n=12).

Supplemental Figure S9. Time course of the net photosynthetic rate (Pn) and cyclic electron flux (CEF) in the 4^{th} leaf as influenced by the suppressed transcript of *RBOH1* in grafted plants.

Supplemental Figure S10. Cyclic electron flux and relative transcript of *ORR* in VIGS plants used for the experiment.

Supplemental Figure S11. CO_2 assimilation rate for WT and phyB plants.

Supplementary Table 1. List of primer sequences used for qRT-PCR analysis.

Supplementary Table 2. Parameters used for detection of IAA and related compound by LC-MS/MS.

Figure 1

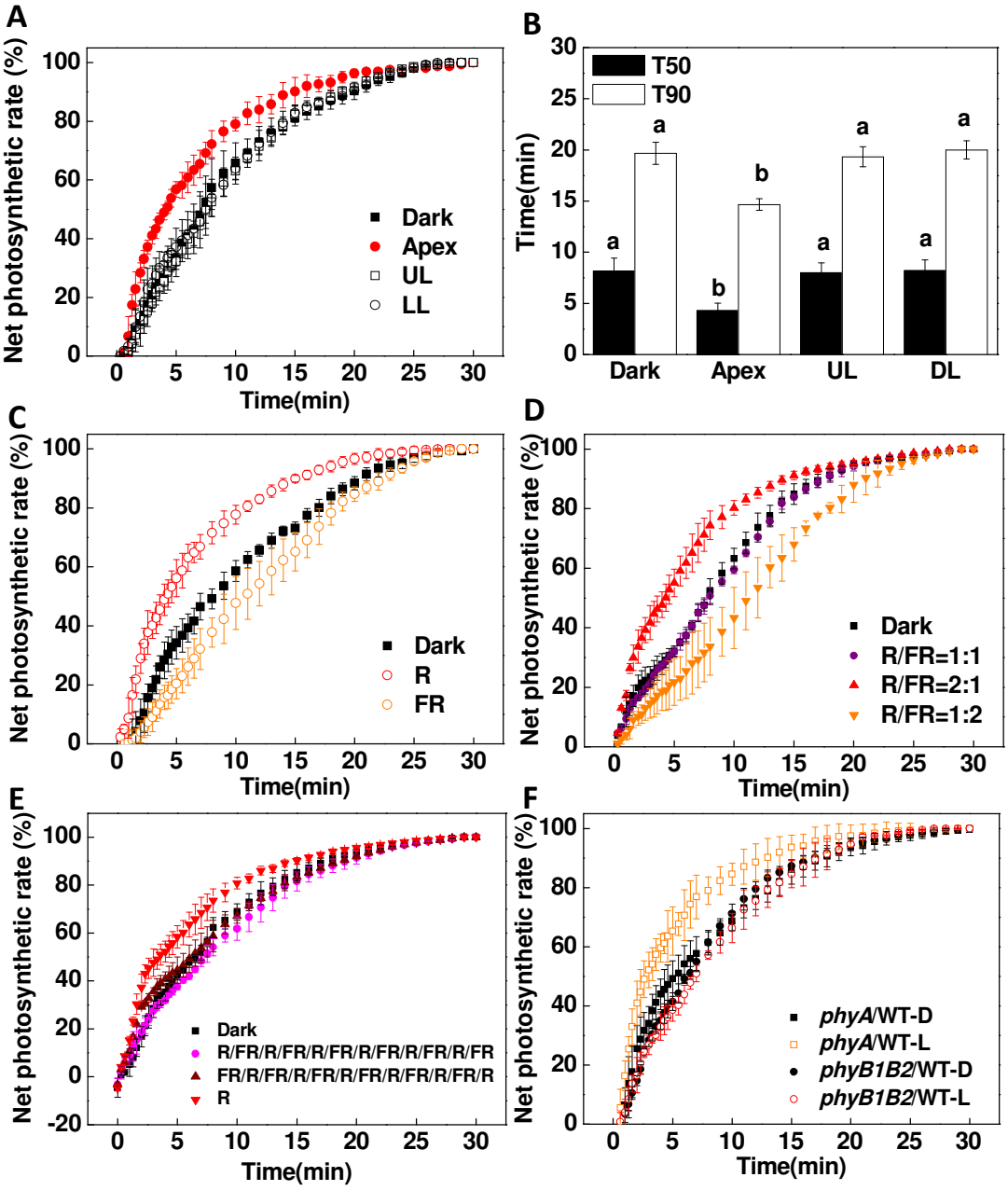
A
Net photosynthetic rate (%)
Time(min)
Dark
Apex
UL
LL
B
Time(min)
T50
T90
a
b
a
a
a
b
a
a
Dark
Apex
UL
DL
C
Net photosynthetic rate (%)
Time(min)
Dark
R
FR
D
Net photosynthetic rate (%)
Time(min)
Dark
R/FR=1:1
R/FR=2:1
R/FR=1:2
E
Net photosynthetic rate (%)
Time(min)
Dark
R/FR/R/FR/R/FR/R/FR/R/FR/R/FR
FR/R/FR/R/FR/R/FR/R/FR/R/FR/R
R
F
Net photosynthetic rate (%)
Time(min)
phyA/WT-D
phyA/WT-L
phyB1B2/WT-D
phyB1B2/WT-L

Figure 2

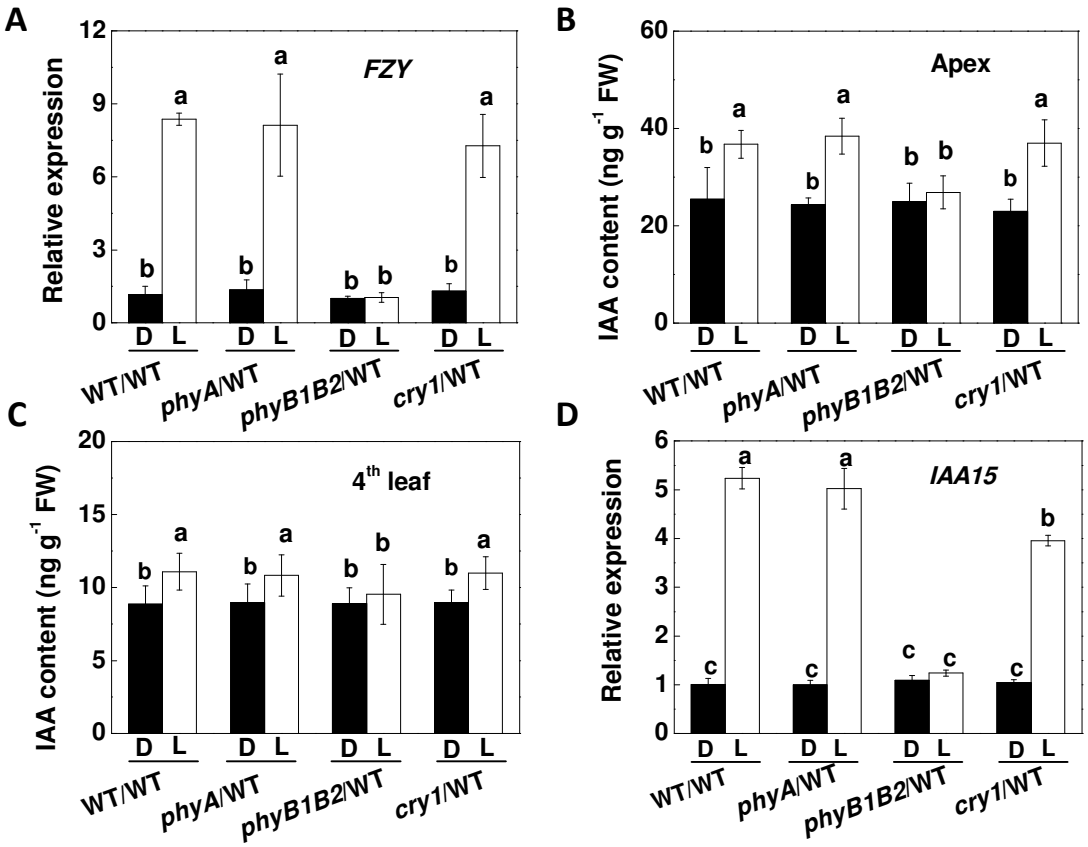
A
FZY
Relative expression
B
Apex
IAA content (ng g-1 FW)
C
4th leaf
IAA content (ng g-1 FW)
D
IAA15
Relative expression
D L
WT/WT
phyA/WT
phyB1B2/WT
cry1/WT

Figure 3

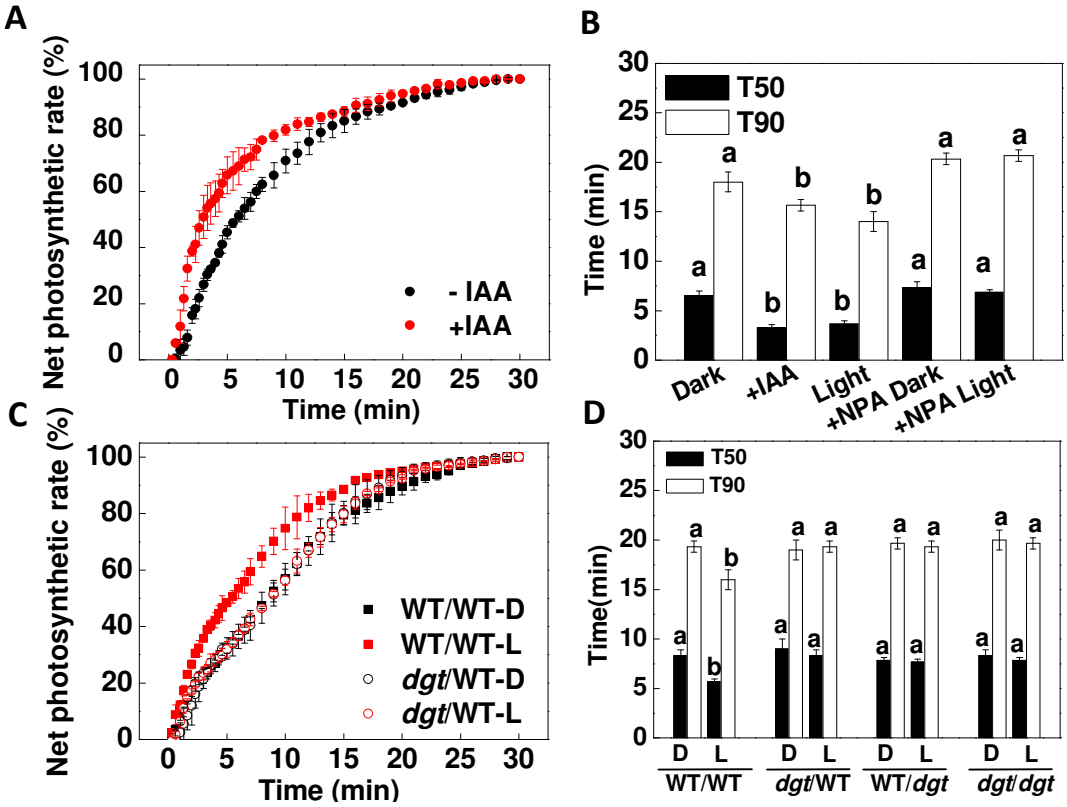
A
Net photosynthetic rate (%)
Time (min)
- IAA
+IAA
B
Time (min)
T50
T90
Dark
+IAA
Light
+NPA Dark
+NPA Light
C
Net photosynthetic rate (%)
Time (min)
WT/WT-D
WT/WT-L
dgt/WT-D
dgt/WT-L
D
Time(min)
T50
T90
D L
WT/WT
dgt/WT
WT/dgt
dgt/dgt

Figure 4

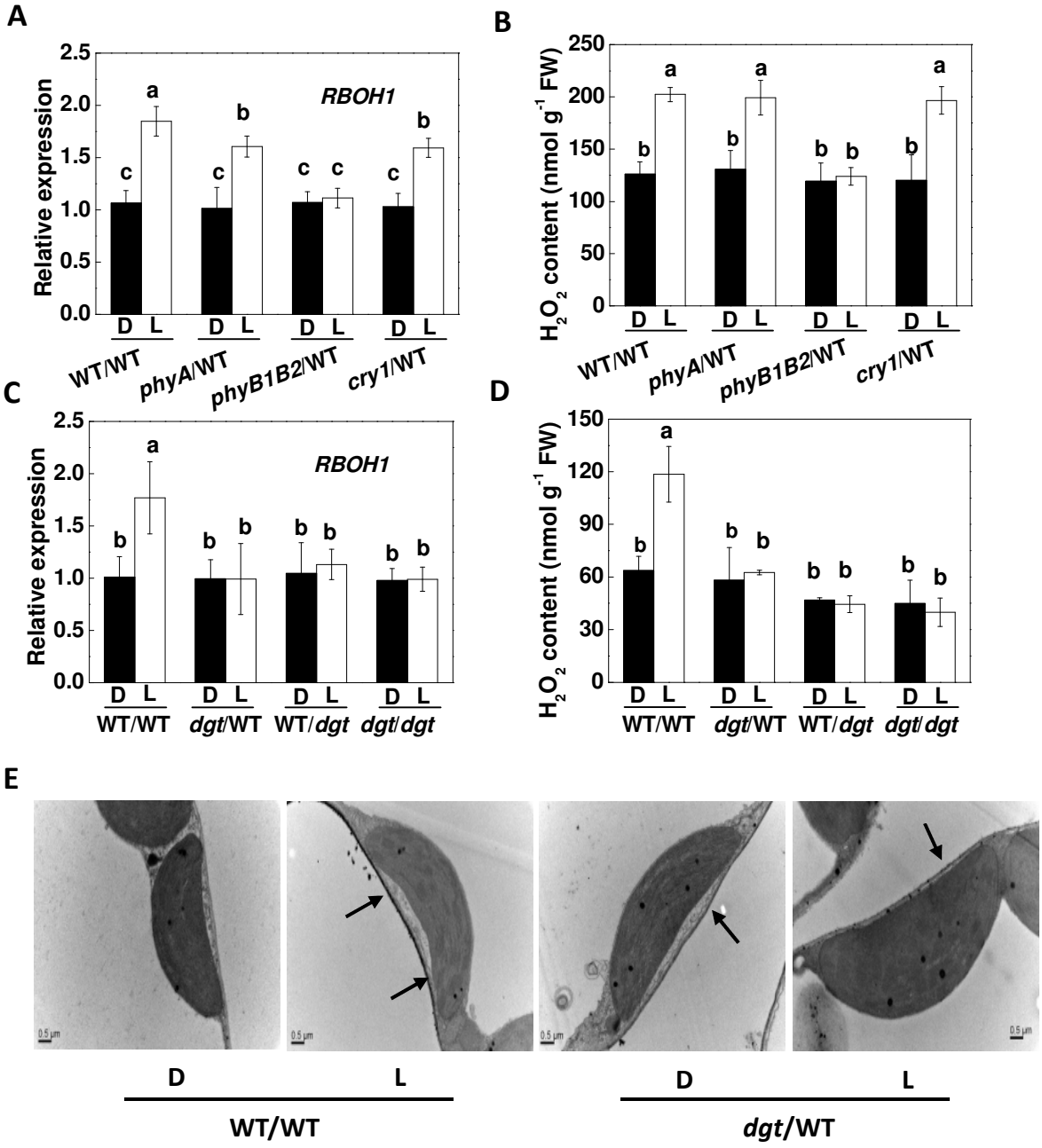
A
Relative expression
RBOH1
D L
WT/WT
phyA/WT
phyB1B2/WT
cry1/WT
B
H2O2 content (nmol g-1 FW)
C
dgt/WT
WT/dgt
dgt/dgt
D
E
WT/WT
dgt/WT

Figure 5

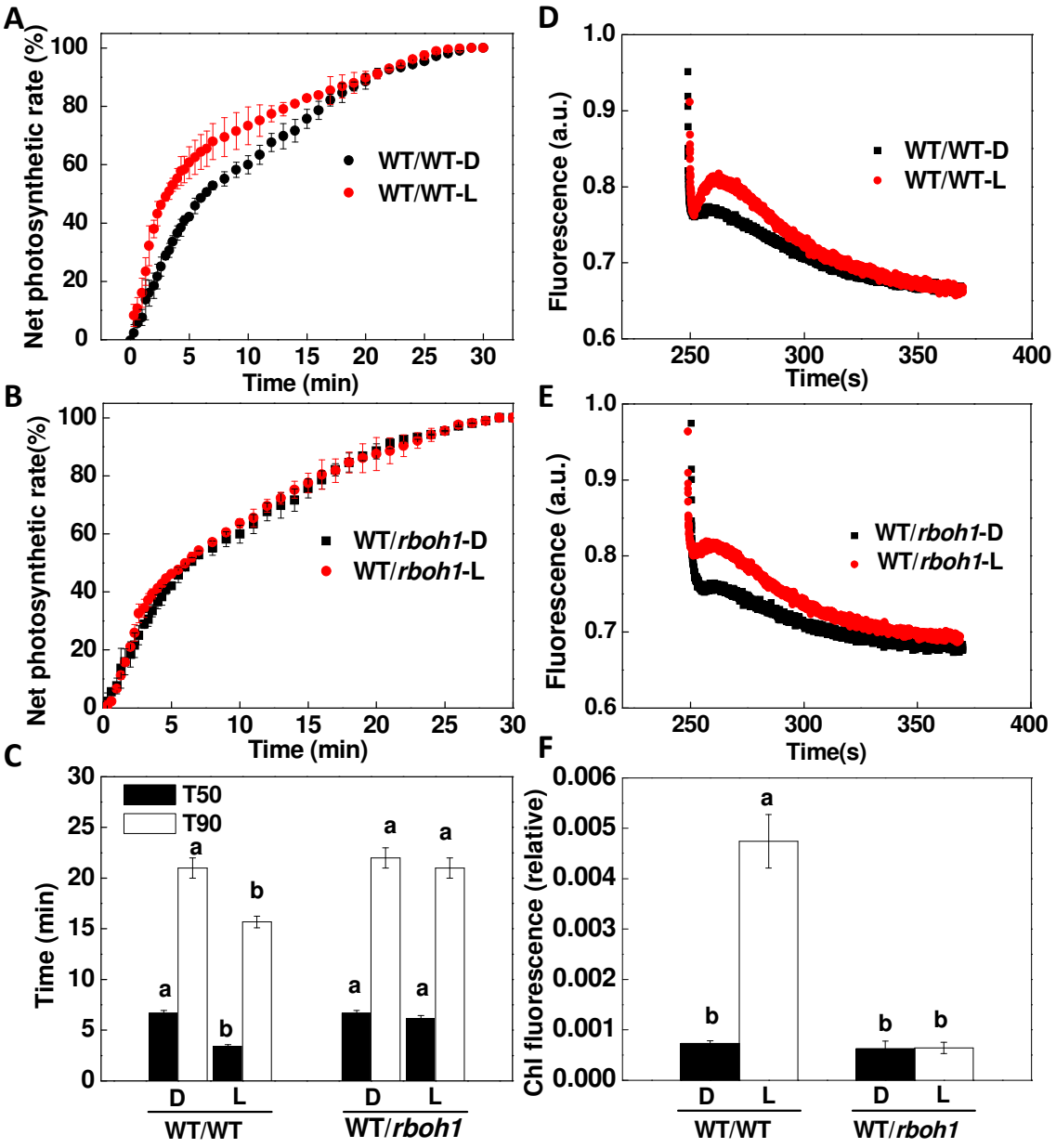
A
Net photosynthetic rate (%)
Time (min)
WT/WT-D
WT/WT-L
B
Net photosynthetic rate(%)
Time (min)
WT/rboh1-D
WT/rboh1-L
C
Time (min)
T50
T90
D
L
WT/WT
WT/rboh1
D
Fluorescence (a.u.)
Time(s)
WT/WT-D
WT/WT-L
E
Fluorescence (a.u.)
Time(s)
WT/rboh1-D
WT/rboh1-L
F
Chl fluorescence (relative)
WT/WT
WT/rboh1

Figure 6

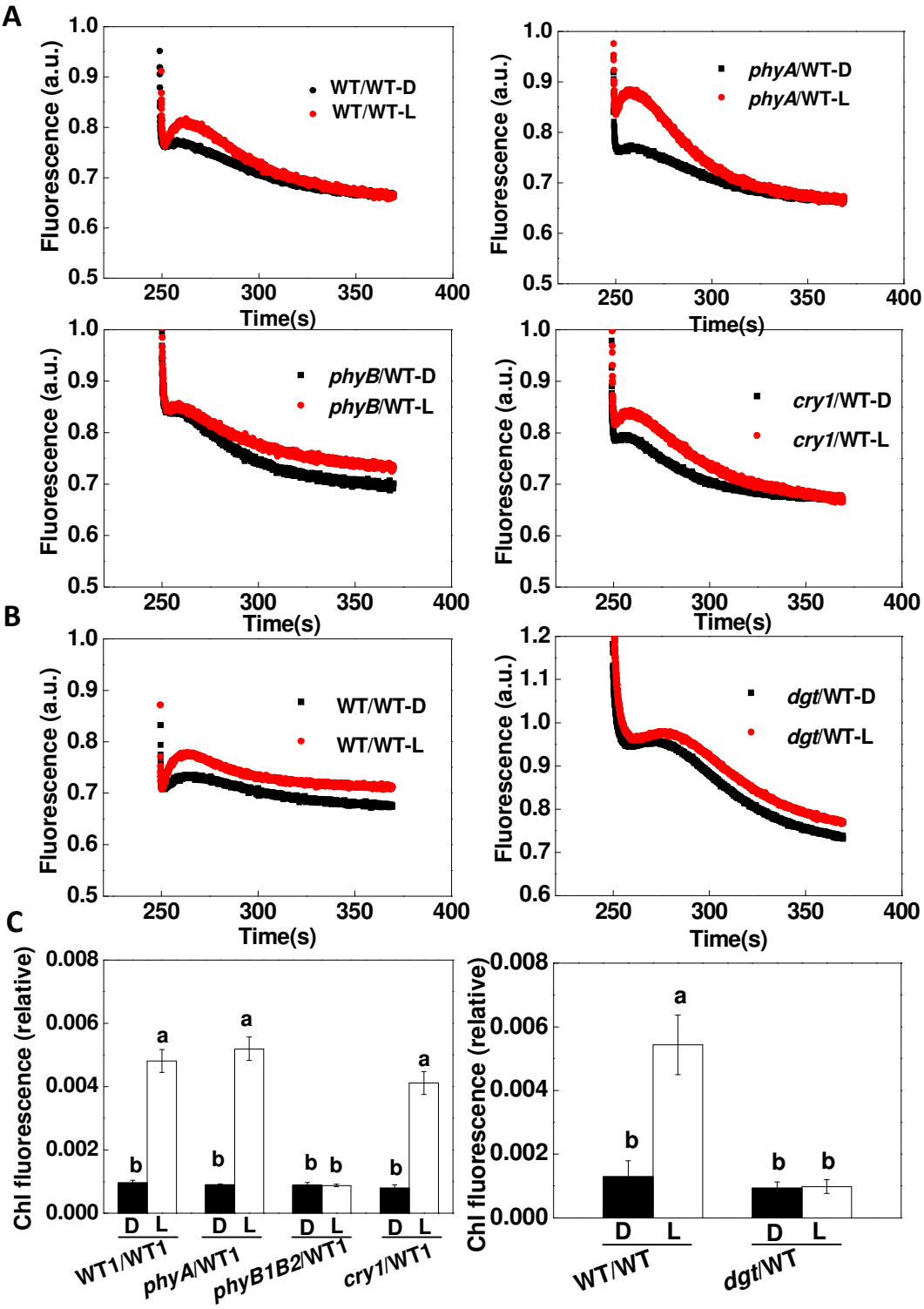
A
Fluorescence (a.u.)
Time(s)
WT/WT-D
WT/WT-L
phyA/WT-D
phyA/WT-L
phyB/WT-D
phyB/WT-L
cry1/WT-D
cry1/WT-L
B
dgt/WT-D
dgt/WT-L
C
Chl fluorescence (relative)
D L
WT1/WT1
phyA/WT1
phyB1B2/WT1
cry1/WT1
WT/WT
dgt/WT

Figure 7

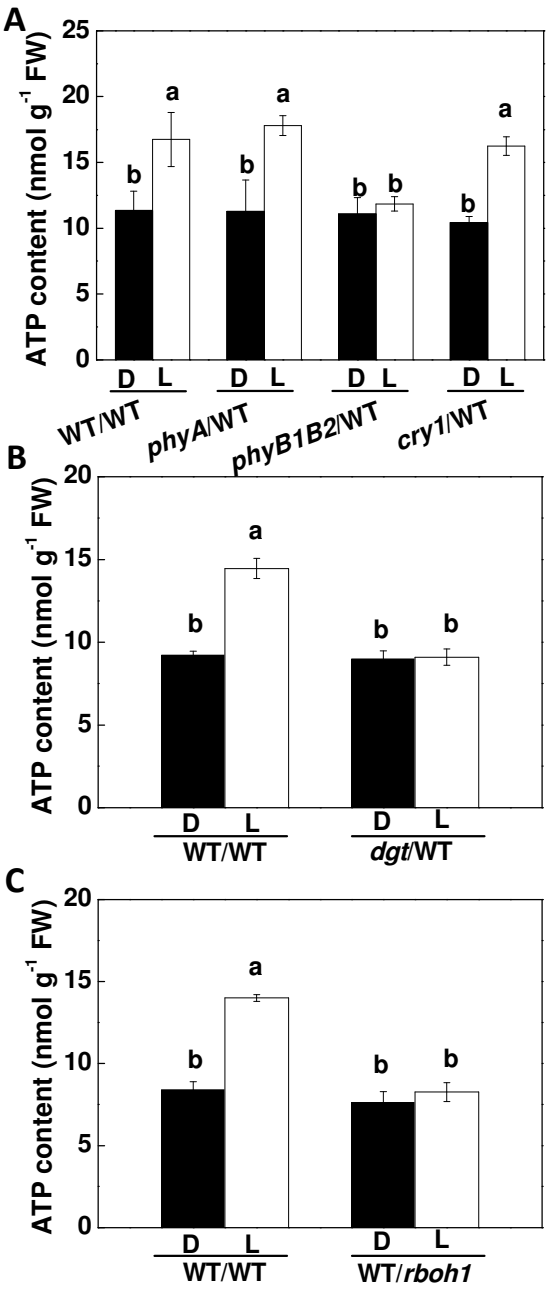
A
ATP content (nmol g-1 FW)
25
20
15
10
5
0
a
a
a
b
b
b
b
b
D L
D L
D L
D L
WT/WT
phyA/WT
phyB1B2/WT
cry1/WT
B
ATP content (nmol g-1 FW)
20
15
10
5
0
a
b
b
b
D L
D L
WT/WT
dgt/WT
C
ATP content (nmol g-1 FW)
20
15
10
5
0
a
b
b
b
D L
D L
WT/WT
WT/rboh1

Figure 8

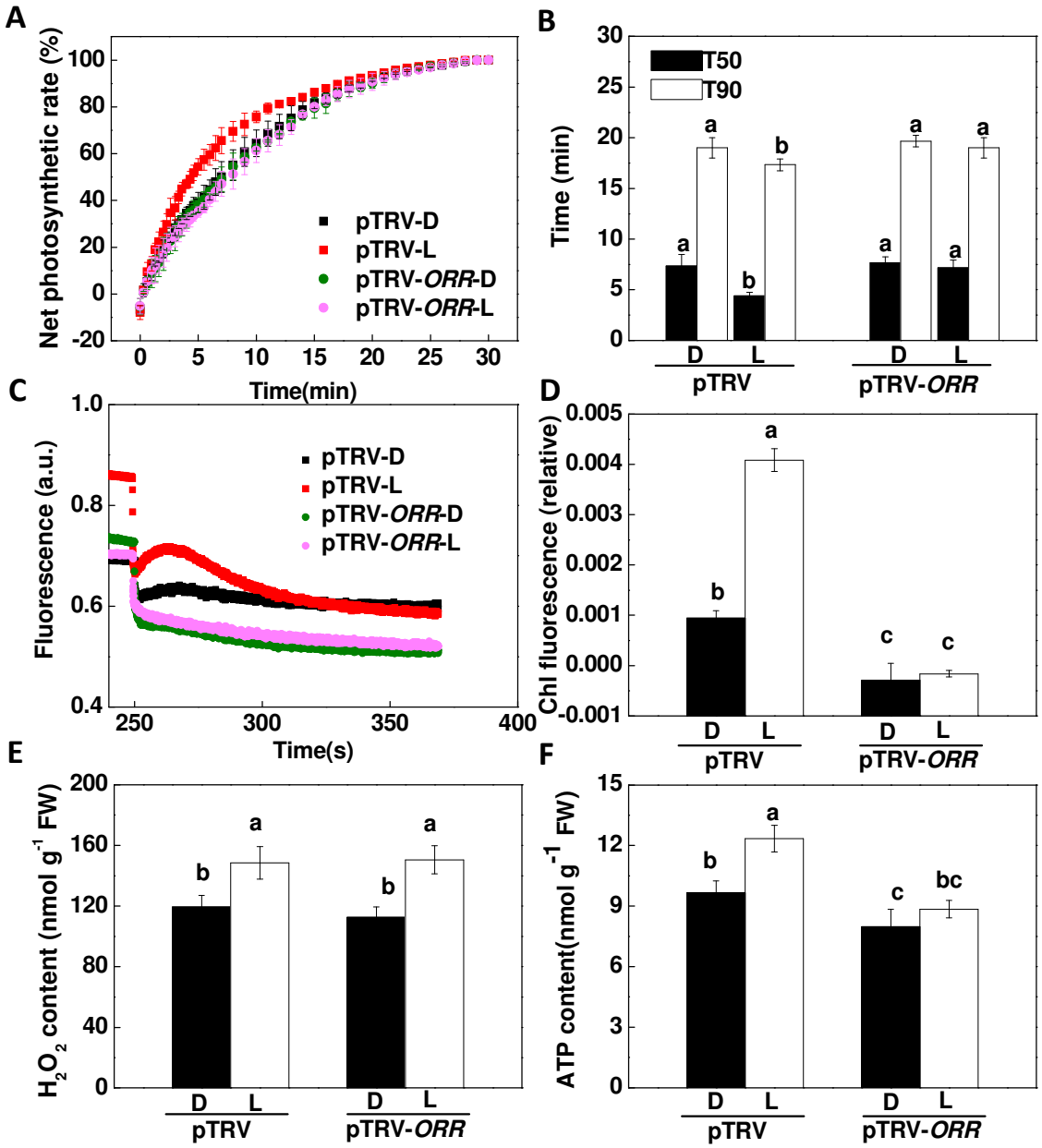
A
Net photosynthetic rate (%)
Time(min)
pTRV-D
pTRV-L
pTRV-ORR-D
pTRV-ORR-L
B
Time (min)
T50
T90
D L
pTRV
pTRV-ORR
C
Fluorescence (a.u.)
Time(s)
pTRV-D
pTRV-L
pTRV-ORR-D
pTRV-ORR-L
D
Chl fluorescence (relative)
E
H2O2 content (nmol g-1 FW)
F
ATP content(nmol g-1 FW)

Figure 9

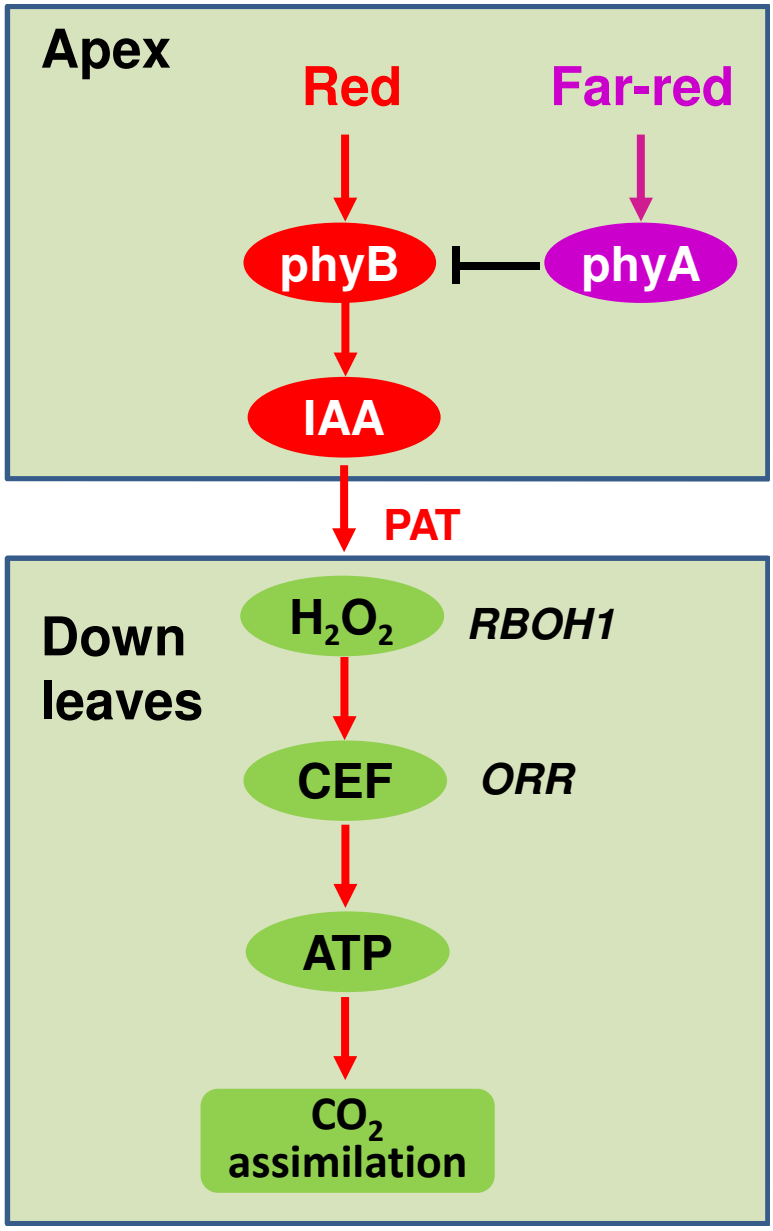
Apex
Red
Far-red
phyB
phyA
IAA
PAT
Down leaves
H_2O_2
RBOH1
CEF
ORR
ATP
CO_2 assimilation